

# A shape memory microcage of TiNi/DLC films for biological applications

Y Q Fu<sup>1,2</sup>, J K Luo<sup>1,3</sup>, S E Ong<sup>4</sup>, S Zhang<sup>4</sup>, A J Flewitt<sup>1</sup> and W I Milne<sup>1</sup>

<sup>1</sup> Department of Engineering, University of Cambridge, Thomson Ave., Cambridge CB0 3FA, UK

<sup>2</sup> Department of Mechanical Engineering, School of Engineering and Physical Sciences, Heriot Watt University, Edinburgh EH14 4AS, UK

<sup>3</sup> Centre for Material Research and Innovation, University of Bolton, Deane Road, Bolton BL3 5AB, UK

<sup>4</sup> School of Mechanical and Aerospace Engineering, Nanyang Technological University, 50 Nanyang Avenue, Singapore 639798

E-mail: [R.Y.Fu@hw.ac.uk](mailto:R.Y.Fu@hw.ac.uk)

Received 26 October 2007, in final form 27 December 2007

Published 6 February 2008

Online at [stacks.iop.org/JMM/18/035026](http://stacks.iop.org/JMM/18/035026)

## Abstract

A TiNi/diamond-like-carbon (DLC) microcage has been designed for biological applications. The structure is composed of a top layer of TiNi film and a bottom layer of highly compressively stressed DLC for upward bending once released from the substrate. The fingers of the microcage quickly close through the shape memory effect once the temperature reaches the austenite start transformation point to execute the gripping action. Opening the microcage is realized by either decreasing the temperature to make use of the martensitic transformation or further increasing the temperature to use the bimorph thermal effect. The biocompatibility of both the TiNi and DLC films has been investigated using a cell-culture method.

(Some figures in this article are in colour only in the electronic version)

## 1. Introduction

Microgrippers are important microtools for biological applications such as biopsy, tissue sampling, cell manipulation, nerve repair and minimal-invasive surgery. The requirements for the microgrippers for such applications include easy operation, low actuation temperature, low operation voltage and low power consumption. A microgripper actuated via high temperature or high voltage damages or even kills living cells or tissues. Most of the microgrippers, such as micro-tweezers, capture micro-objects by applying a force directly to the subject, which may easily cause damage to the subject. A microcage, on the other hand, captures the micro-object by confining or trapping it without applying a force directly on it, thus avoiding the potential damage to the tissues or cells. A microcage with multiple fingers of a bimorph structure can be fixed on a multi-degrees-of-freedom robotic arm to capture, transport and manipulate bio-cells for dissection and injection.

Microactuation for manipulating the tissue, cells or other biological subjects can be realized by optical, electrical, piezoelectric, dielectric, mechanical, thermal, pneumatic and electromagnetic methods [1–5]. Compared to these

mechanisms, a thin film shape memory alloy is promising in microgripper and microcage applications for its high power density (up to  $10 \text{ J cm}^{-3}$ ), low actuation temperature (50 to  $80^\circ\text{C}$ ), ability to recover large transformation stress and strain upon heating and cooling, pseudoelasticity (or superelasticity) and biocompatibility [6–8].

Diamond-like-carbon (DLC) is a promising material for MEMS applications [9, 10]. DLC is biocompatible, mechanically and tribologically strong, thus is an excellent coating material for implantable medical devices. It has a large Young's modulus, excellent thermal conductivity and a low coefficient of thermal expansion (CTE), all of which are useful in developing bimorph thermal actuators with large displacements. In [11], we successfully fabricated a closed multi-finger microcage based on the electroplated nickel and DLC bimorph structure with dimensions down to bio-cell sizes of  $\sim 40 \mu\text{m}$ . A highly compressively stressed (a few GPa) DLC layer expands and lifts the bimorph structure upward once it is released from the substrate, forming a closed microcage [11]. The device can be opened by pulsed current in a millisecond at a power of a few tens of milliwatts. However, the operation temperature of that Ni/DLC microcage is too high ( $300\text{--}400^\circ\text{C}$ ) for the practical biological applications. Theoretical

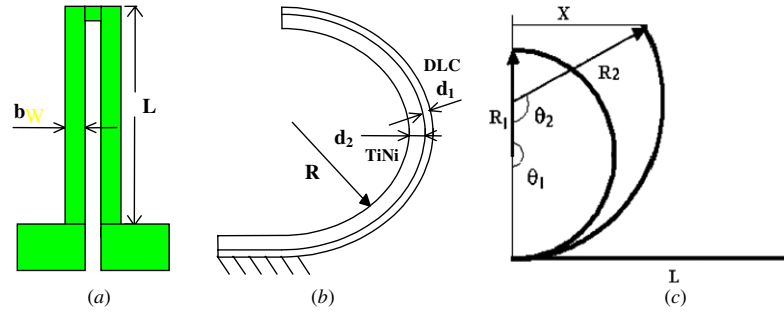


**Figure 1.** Schematic drawing of bimorph TiNi/DLC microfinger structures: (a) top view; (b) cross-section view after bending up and (c) illustration of bending angular and displacement.

analysis revealed that the operation temperature of the bimorph microcage is inversely proportional to the difference in CTEs of the two-layer materials [11]. In order to reduce the operation temperature, it is necessary to select two materials with large difference in CTEs, such as DLC and polymer. Based on this analysis, a microcage with a SU-8/Al/DLC trilayer design has been fabricated [12], and experimental results confirmed that the temperature for operation can be lowered down to about 100 °C. Further reduction in the operation temperature of the microcage can be realized by using shape memory effect. TiNi-based thin film shape memory alloys have advantages such as large displacement and force generation, transformation temperatures less than 80 °C and good biocompatibility. These properties make the TiNi shape memory thin films promising for microcage applications [13–17]. In this study, a TiNi/DLC bimorph microcage structure has been designed, analyzed, fabricated and characterized. Cell culture has been performed *in vitro* to determine the cellular behavior on both DLC and TiNi films.

## 2. Microcage design considerations

A schematic TiNi/DLC bimorph microfinger structure is shown in figure 1. The DLC film has a large compressive stress, and the TiNi film at room temperature (i.e., in martensite state) normally shows small tensile stress. When the DLC is used as the bottom layer and TiNi as the top layer of the bimorph structure, significant upbending of the fingers of the microcage could occur when it is released from the Si substrate. The radius of curvature,  $R$ , of the bimorph TiNi/DLC structure (shown in figure 1(b)) after being released from the Si substrate can be controlled by changing the thickness ratio of the two layers, or by changing the stress state in both the TiNi and DLC layers [11, 18]:

$$\frac{1}{R} = \frac{6 \times \varepsilon_{eq}(1+m)^2}{d[3(1+m)^2 + (1+mn)(m^2 + (mn)^{-1})]} = \varepsilon_{eq} \times M \quad (1)$$

where  $M$  is a dimension-related parameter and  $\varepsilon_{eq}$  is the equivalent strain. Because the as-deposited TiNi film has a very low tensile stress, it is assumed that strain change of the bimorph structure is dominated by the DLC layer. Assuming that stress is uniaxial (since the bimorph is slender), the equivalent strain  $\varepsilon_{eq}$  in the DLC layer can simply be calculated

using the as-deposited stress  $\sigma_d$  and Young’s modulus  $E_d$  of the DLC layer, i.e.,  $\varepsilon_{eq} = \sigma_d/E_d$ . In equation (1),  $d = d_1 + d_2$ , in which  $d_1$  and  $d_2$  are the thicknesses of the DLC and TiNi layer respectively,  $n (=E_1/E_2)$  and  $m (=d_1/d_2)$  are the ratios of Young’s modulus and the layer thickness of the two layers.  $M$  is a constant for the fixed materials and structural configuration. Equation (1) implies that once the materials and layer thickness are fixed, the radius of curvature can be adjusted by varying the stress and strain of both the top TiNi layer and bottom DLC layer, which can be realized using different deposition methods and/or different process conditions [11].

During thermal cycling, the opening/closing performance of the microcage is mainly determined by (1) thermal effect: temperature change and the difference in the CTEs of the two materials and (2) shape memory effect. First, we analyze the curvature changes due to pure thermal effect. If the temperature of the bimorph finger increases from  $T_1$  to  $T_2$ , due to the difference of the CTE between the TiNi and DLC, the thermal expansion mismatch leads to the TiNi layer expanding more than the DLC layer, thus opening the microcage and changing the radius of curvature from  $R_1$  to  $R_2$ . The thermal strain,  $\varepsilon_{th}$ , generated through resistive Joule heating of the bimorph layer is expressed as  $\varepsilon_{eq} = (\alpha_d - \alpha_{TiNi}) \times \Delta T$ , where  $\alpha_d$  and  $\alpha_{TiNi}$  are the CTEs of the DLC and TiNi, respectively. The radius of the curvature  $R$ , the bending angle  $\theta$  (in degree) and the length of the finger  $L$  have the following relationship (see figure 1(c)) [11]:

$$\theta = \frac{180^\circ \times L}{\pi \times R} \quad (2)$$

Combining equations (1) and (2), the angle change from  $\theta_1$  (refers to the initial degree of bending at room temperature) to  $\theta_2$  (a new position) due to the pure thermal effect from a temperature change ( $\Delta T = T_2 - T_1$ ) becomes [11]

$$\begin{aligned} \Delta\theta = \theta_2 - \theta_1 &= \frac{180^\circ \times L}{\pi} \left( \frac{1}{R_2} - \frac{1}{R_1} \right) \\ &= \frac{180^\circ \times L}{\pi} \Delta\varepsilon_{thermal} \cdot M = \frac{180^\circ \times L}{\pi} \Delta\alpha \Delta T M \quad (3) \end{aligned}$$

where  $M$  is a dimension parameter as listed in equation (1). According to the design, the finger lengths are 50, 100 and 150  $\mu\text{m}$ . The thickness of the DLC layer is 100 nm and the thickness of the TiNi layer is 800 nm. The stress of the as-deposited DLC film was determined to be 5 GPa.

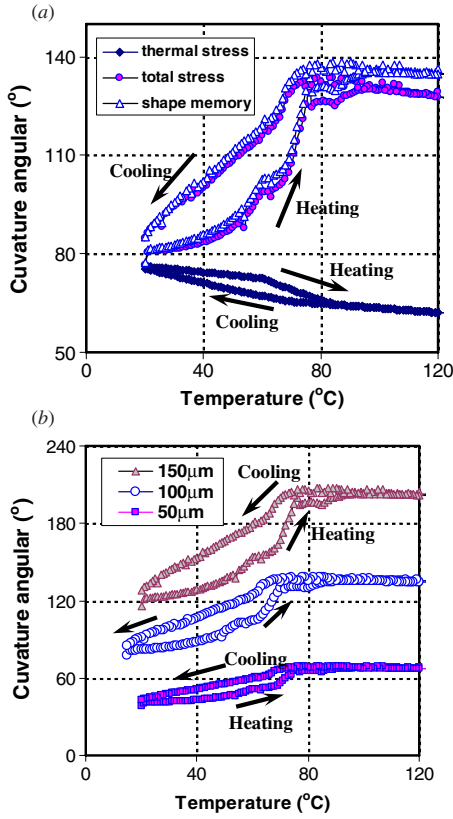


**Figure 2.** Comparison of curvature angular changes (a) due to the total stress evolution, thermal effect, shape memory effect for the TiNi/DLC microfinger with a beam length of 100  $\mu\text{m}$  and (b) beam lengths of 50, 100 and 150  $\mu\text{m}$ .

In calculation, the elastic modulus and thermal expansion coefficient of the TiNi film is a variable which is a function of temperature, based on the rule of mixtures depending on the percentage of martensite/austenite at a given temperature. The CTE of the DLC is  $1 \times 10^{-6} \text{ K}^{-1}$ . The elastic moduli of martensite and austenite of the TiNi film are chosen as 30 GPa and 75 GPa and the CTEs of martensite/austenite of the TiNi films are  $11 \times 10^{-6} \text{ K}^{-1}$  and  $9 \times 10^{-6} \text{ K}^{-1}$ , respectively [7, 8]. Young's modulus of DLC is  $\sim 600 \text{ GPa}$  [11]. The calculated results are shown in figure 2. The bending angle decreases slightly with the increase of temperature during heating, indicating that the microfingers slightly open owing to bimorph thermal effect. A hysteresis is observed during the thermal cycle due to differences in forward and martensitic transformations upon heating/cooling (i.e., different contents of martensite and austenite at a certain temperature during thermal cycling).

To calculate the curvature change of the bimorph structure due to shape memory effect, the stress evolution of the TiNi film on the Si substrate as a function of temperature was measured (see figure 3). The stress versus temperature plot shows a closed hysteresis loop after the heating and cooling process: a sharp increase in tensile stress is seen in response to the phase transformation from martensite to austenite upon heating; upon cooling, the stress relaxes significantly

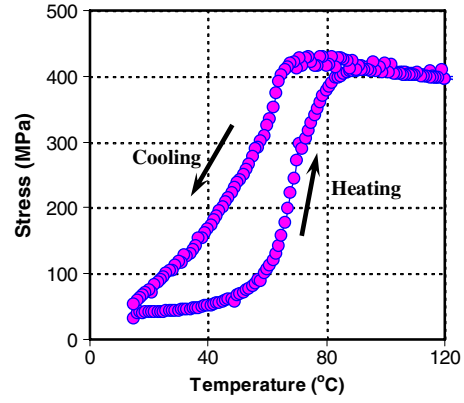


**Figure 3.** Stress evolution as a function of temperature for the TiNi film on the silicon substrate.

corresponding to the formation of a twinning structure due to martensitic transformation [6]. Since the thermal stress also contributes to the stress evolution of the TiNi/Si structure, the stress evolution due to pure shape memory effect can be obtained by deducting the thermal stress (for the TiNi/Si system shown in figure 2) from the total stress evolution shown in figure 3. Substituting into equation (1) the stress change induced by shape memory effect gives rise to the estimation of the angle changes of the finger due to shape memory effect:

$$\begin{aligned} \Delta\theta_{\text{SME}} &= \frac{180^\circ \times L}{\pi} \Delta\varepsilon_{\text{SME}} \times M \\ &= \frac{180^\circ \times L}{\pi} \left( \frac{\Delta\sigma_{\text{total}}}{E_{\text{TiNi}}/(1-\nu)} - \Delta\alpha \times \Delta T \right) M. \end{aligned} \quad (4)$$

The CTE of Si is  $2.6 \times 10^{-6} \text{ K}^{-1}$ . Figure 2(a) shows the estimated curvature angular changes of the TiNi/DLC microfinger due to shape memory effect as well as total stress (for microfinger with a length of 100  $\mu\text{m}$ ). The curvature angular changes significantly (about  $60^\circ$  in angle) as temperature increases from room temperature to 80  $^\circ\text{C}$ . During heating, the bending angle increases with temperature indicating that the fingers of the microcage close, which is opposite to the opening movement caused by the thermal effect (figure 2(a)). Clearly, the shape memory effect dominates the microfinger deformations within this temperature range and the contribution from the thermal bimorph effect is negligible. Figure 2(b) shows the effects of the finger length on the curvature angle changes during a thermal cycle. The longer the finger beam is, the larger the initial bending curvature angle after the release from the Si substrate, and more significant changes in curvature angular during heating/cooling.

From the results shown in figure 2(a), it is predicated there will be two possible curvature changes during heating/cooling. At initial heating, there will be an insignificant opening of microcage fingers due to thermal effect. When heated above austenite start transformation temperature, the microfingers close significantly due to shape memory effect, which executes the action of capturing the micro-object. Opening of the microcage can be realized by either decreasing the temperature (due to the martensitic transformation) or by further increase in temperature (thermal bimorph effect, but it may need very high temperature, thus is not desirable for practical application).

A rough estimation according to equation (1) indicates that if the thickness ratio of TiNi/DLC is 1, there will be a maximum bending effect. However, the thickness of TiNi should be larger than a few hundred nanometers, below which the shape memory effect will be too weak for an efficient actuation [19]. When the film is too thin, surface oxide and film/substrate interfacial diffusion layers exert dominant constraining effect that renders high residual stress and low recovery capabilities [19, 20]. The surface oxide and inter-diffusion layer restricts the phase transformation, alters the chemical stoichiometry of the remaining TiNi film, which effectively reduces the volume of the material available for phase transformation. It was reported that a maximum recovery stress and actuation speed can be realized with a TiNi film thickness at about 1  $\mu\text{m}$  [19]. On the other hand, there is also a limit to the DLC thickness. When the thickness of DLC is above 100 nm, the DLC layer may peel off from the Si substrate due to intrinsic stress. This has severely restricted the usage of DLC of a few hundred nm thick.

### 3. Microcage fabrication and characterization

Microcages of five, six and seven fingers were designed. The width of the fingers and the gap between the beams were 4  $\mu\text{m}$ . The fingers were connected to each other with bond pads. The central part of the microcage was large enough so that it remained attached to the substrate after the fingers were released from the substrate. A DLC film of 100 nm was deposited on the Si substrate using a filtered cathodic vacuum arc (FCVA) method with a graphite source. The compressive stress of the film was 5 GPa as determined via the curvature measurement. A TiNi film of 800 nm thick was deposited on top of the DLC layer by magnetron sputtering in an argon gas environment at a pressure of 0.8 mTorr from a  $\text{Ti}_{50}\text{Ni}_{50}$  target (using a 400 W rf power) and a 99.99% pure Ti target (using a 70 W dc power). Post-annealing of the TiNi/DLC bimorph layer was performed at 480  $^{\circ}\text{C}$  for 30 min in a high vacuum condition for crystallization.

The DLC/TiNi microcage was fabricated by photolithographically patterning of a 4.8  $\mu\text{m}$  thick AZ4562 photoresist on top of the TiNi films. An  $\text{HF:HNO}_3:\text{H}_2\text{O}$  (1:1:20) solution was employed to etch the TiNi films to form the microcage patterns. The exposed DLC underlayer was etched off in oxygen plasma at a flow rate of 80 sccm and a power of 100 W. A deep reactive ion etching machine was used to isotropically etch the silicon substrate with  $\text{SF}_6$  plasma at a flow rate of 70 sccm and pressure of 72 mTorr. The coil and platen powers were set at 50 W and 100 W, respectively. A time controlled etching was performed to release the fingers leaving the middle parts of the microcage remained attached to the Si substrate. The actuation performance of the released microgrippers was evaluated using a Peltier device (with a temperature range from 5  $^{\circ}\text{C}$  to 100  $^{\circ}\text{C}$ ) in this preliminary study. The displacements of the TiNi pattern were measured using a video camera from the top view.

SEM morphology of the fabricated TiNi/DLC microcages on a 4 inch silicon wafer is shown in figure 4(a). The microcages have different finger numbers and lengths. After

being released from the Si substrate, the microcages show significant curling up of the microfingers, depending on the beam lengths. The seven-finger microcages with different beam lengths are shown in figures 4(b)–(e). As designed, with the increase of the beam length, the microfingert patterns of the microcages change from fully open, under-closed to over-closed (see figures 4(b)–(e)). Figure 5 shows the top-view optical images of the deformation behavior of a five-finger microcage upon heating. Actuation of the microcage is mainly determined by shape memory effect. With temperature increased above austenite start transformation temperature (about 50 to 60  $^{\circ}\text{C}$ ), martensite changes to austenite, causing the closing of microcages and capturing an object (see figures 5(b)–(d)). Further increase in temperature above 100  $^{\circ}\text{C}$  causes slight opening of the microfingers due to thermal effects. Upon cooling, the microcage fingers quickly open due to the martensitic transformation. Figures 6(a) and (b) show the top-view optical images of a seven-finger microcage at room temperature and after heating, also showing a dramatic closing/opening of the microcage during heating/cooling. As one example for the real application, figure 7 shows an SEM image of the microcage capturing a polymer microsphere with a diameter of 50  $\mu\text{m}$ .

Based on the calculation results of the curvature angular change for the beams with different lengths shown in figure 2(b), the microfingert displacement in the horizontal direction can be estimated from the simplified relationship:  $\sin(180 - \theta) = \frac{x}{R} = \frac{x \times \theta}{L}$ , and the results are shown in figure 8(a). Beam length has a dramatic influence on the opening displacement in the  $x$ -direction. Figure 8(b) plots the experimentally measured changes in the horizontal displacement of a microcage fingertip (beam length of 150  $\mu\text{m}$ ) as a function of substrate temperature. Horizontal displacements of 50 to 60  $\mu\text{m}$  can be achieved at temperatures less than 80  $^{\circ}\text{C}$ . The theoretical calculated results are comparable with the experimental measured results as shown in figure 8(b). However, there is a discrepancy between the estimated and the measured results. Several reasons are possible for this discrepancy: (1) in a theoretical calculation, the stress–temperature results measured from a film on a 4 inch Si wafer were used. However, the real stress–temperature relationship could be different from that on the TiNi/DLC bimorph structure. (2) In measurement, the temperature of the fingers of the microcage should be lower than those measured on the surface of the Peltier device. (3) During the fabrication of DLC/TiNi microcages, a post-annealing crystallization process was used which could have relaxed some of the DLC stress. Also the plasma releasing of the microfingert from the silicon substrate could deteriorate the shape memory effect of a TiNi film due to plasma damage on the surface of the material. These effects should be considered when designing the microcages for practical usages.

The fabricated microcage has been thermally cycled between 20  $^{\circ}\text{C}$  and 100  $^{\circ}\text{C}$  for several hundred cycles and optical microscopy observation did not reveal apparent degradation. Further experimental work is being performed to measure the tip displacement produced by passing a current through the TiNi electrode as a function of the voltage amplitude and frequency.

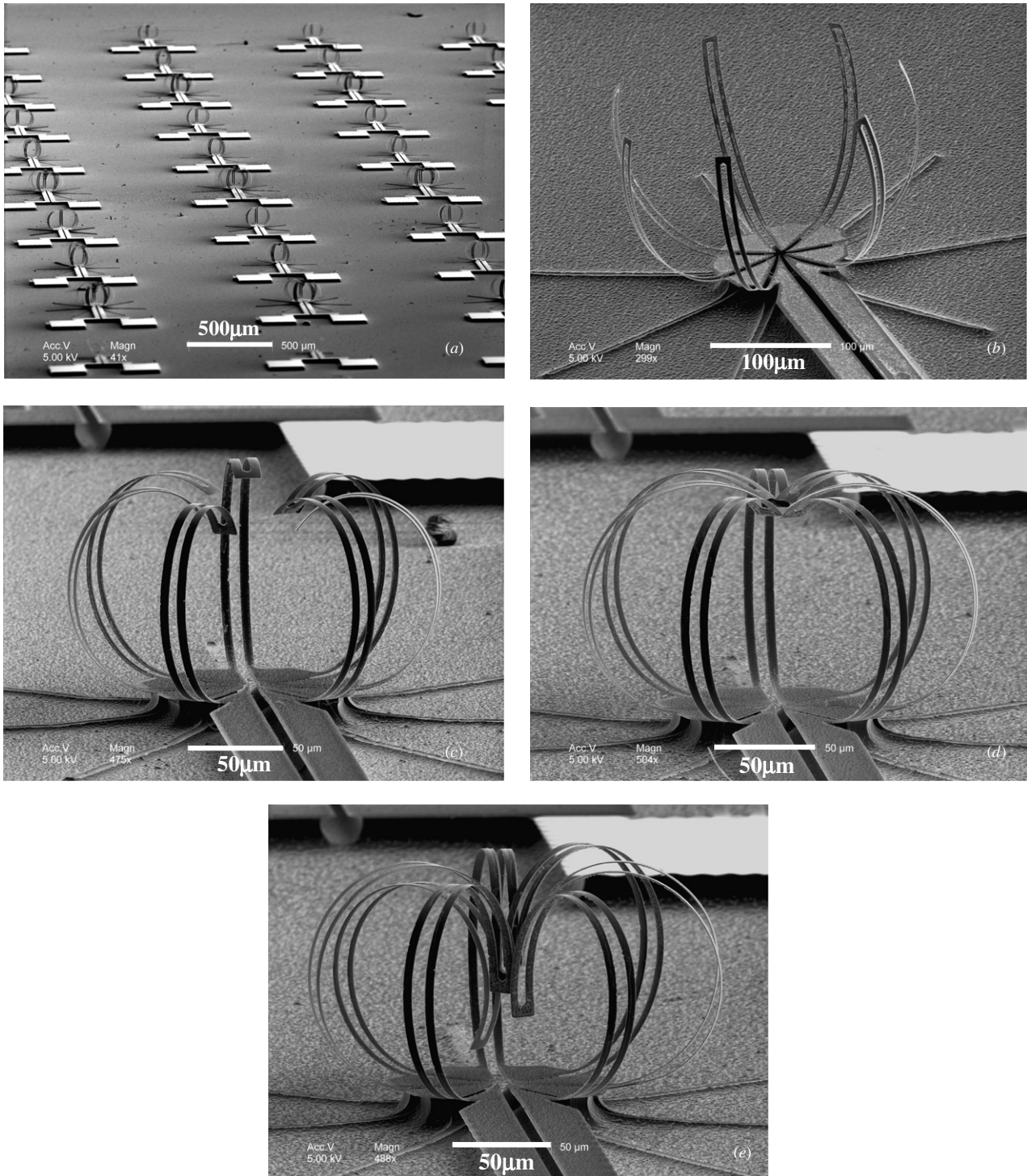


**Figure 4.** TiNi bending-up microcage structure (a) on a 4 inch wafer with different finger lengths; (b) 100 μm; (c) 120 μm; (d) 180 μm; (e) 200 μm.

In biological evaluation, a cell culture assay was performed on both the TiNi and DLC films. The cell line used for the assay was COS7 (African green monkey kidney fibroblast) obtained from American Type Culture Collection (ATCC, Rockwell, MD). The autoclave-sterilized samples

(10 mm × 10 mm) were placed in a 24-well plate for fibroblast seeding at a set density of  $1.4 \times 10^4$  cells ml<sup>-1</sup>. The cells were incubated in Dulbecco's modified Eagle's medium supplemented by 10% fetal calf serum and 1% penicillin for a total period of 6 days. The incubation was carried out at

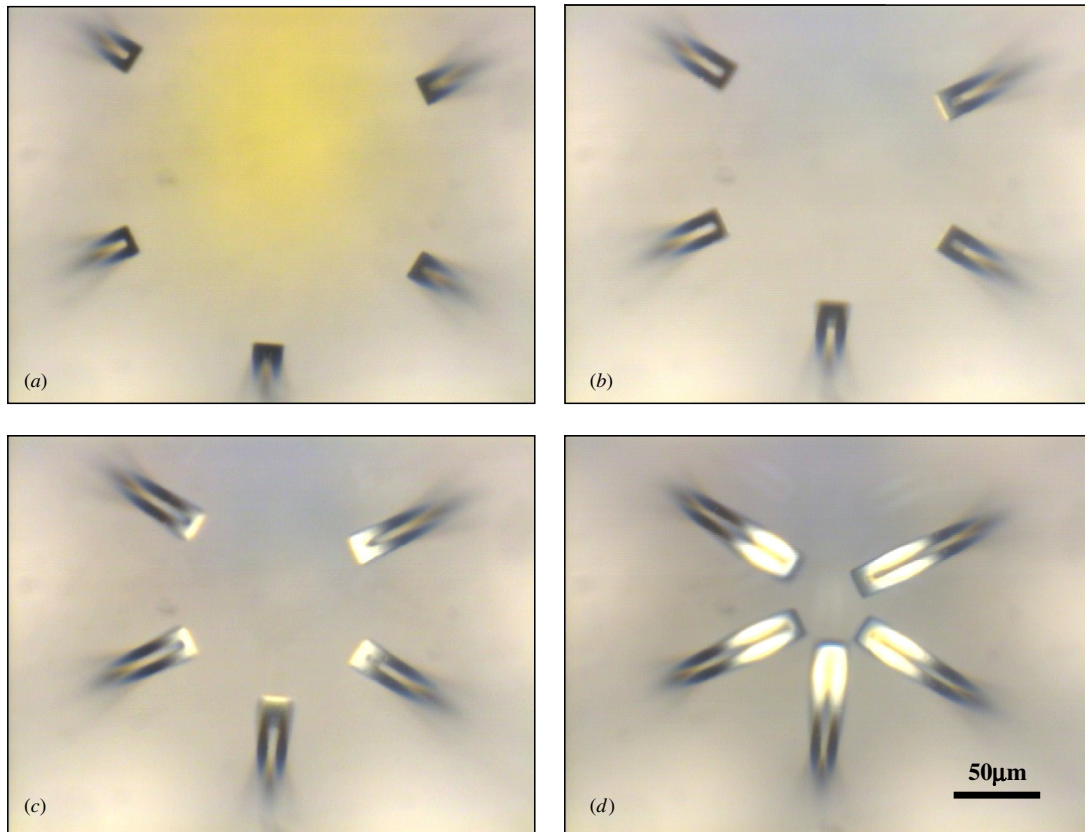


**Figure 5.** Optical microscopy images showing the closing of a five-finger microcage during heating (during cooling the process is reversed; beam length:  $150\ \mu\text{m}$ ): (a)  $20\ ^\circ\text{C}$ , (b)  $55\ ^\circ\text{C}$ , (c)  $65\ ^\circ\text{C}$  and (d)  $80\ ^\circ\text{C}$ .

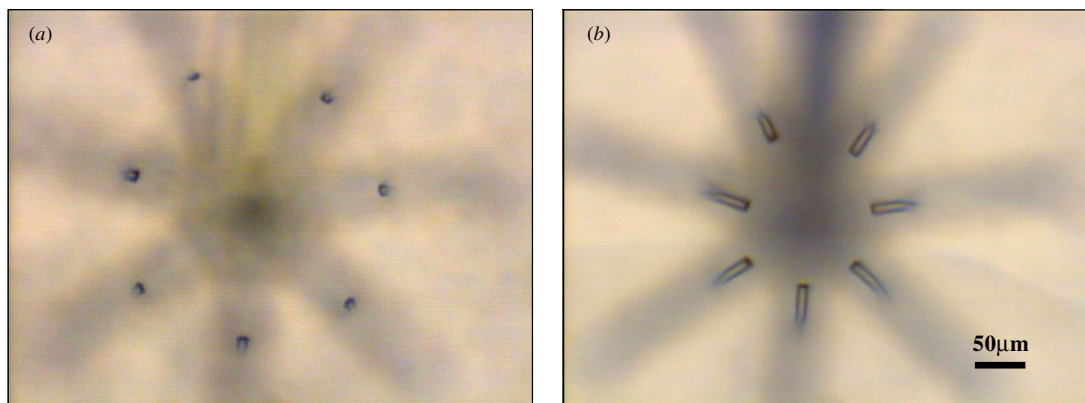


**Figure 6.** Optical microscopy images showing the opening/closing of a microcage during heating (during cooling the process is reversed; beam length:  $100\ \mu\text{m}$ ): (a)  $20\ ^\circ\text{C}$  and (b)  $80\ ^\circ\text{C}$ .

$37\ ^\circ\text{C}/5\% \text{CO}_2$  in air in a humidified incubator. The cells were trypsinized to detach them from the sample surface. After being extracted from the culture plate, the cells and medium mixture were centrifuged in order to separate them. The supernatant was removed and 1 ml of fresh medium was added.  $20\ \mu\text{l}$  of cell suspension was then mixed with  $180\ \mu\text{l}$  of Trypan Blue, and injected into the chambers of a hemacytometer for counting. Three replicated samples were processed for each coating. For the cell morphology observation, the fibroblasts

attached on the coatings were fixed with 2.5% glutaraldehyde for 30 min, and then dehydrated.

Figure 9 shows the fibroblast cell attachment on both the TiNi and DLC film surfaces after 2 day incubation. Well-attached and proliferated cells can be observed, indicating a fast proliferation and healthy behavior of the cells. Analysis of variance (ANOVA) is used to determine if the growth is actually a true proliferation. This is conducted for the counts at different durations up to 6 days for the TiNi and DLC films.

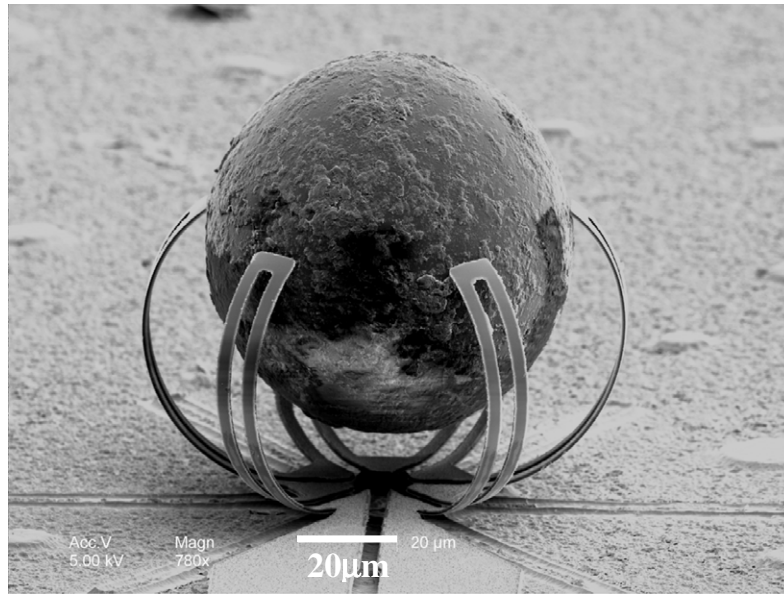
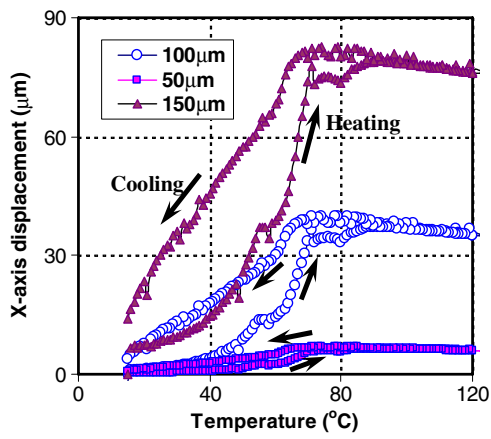
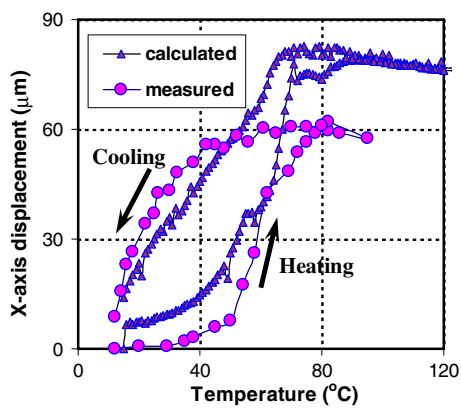


Figure 7. SEM picture of a microcage capturing a micro-polymer ball.



(a)



(b)

Figure 8. Horizontal displacement as a function of temperature for a microfinger: (a) with different finger lengths and (b) experimental measured results and calculated results with a finger length of 150  $\mu\text{m}$ .

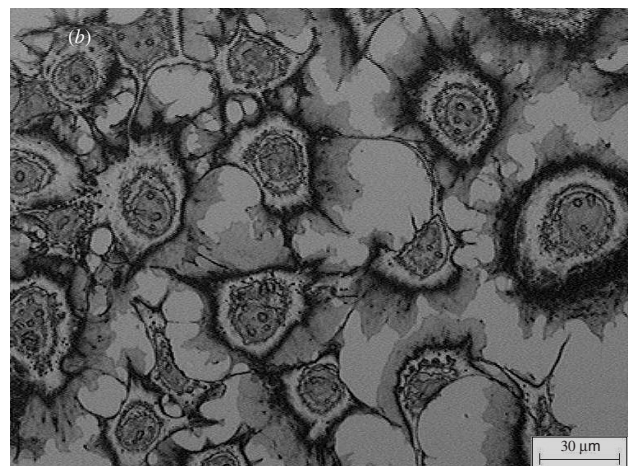
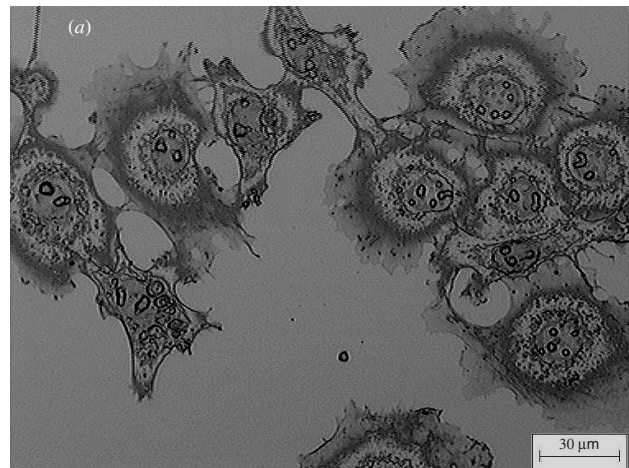
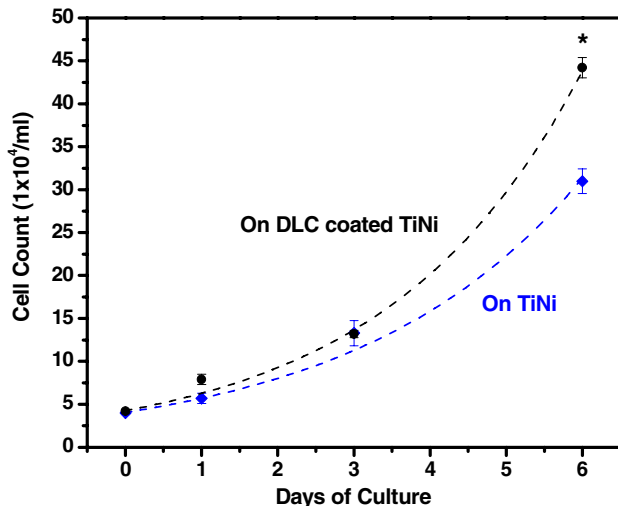


Figure 9. Typical morphology of cells attached on surfaces of (a) TiNi and (b) DLC.



**Figure 10.** Cell growth curve on TiNi and DLC coated TiNi surfaces. \* denotes significant difference from TiNi.

Results in figure 10 showed that the cells are truly proliferating on both surfaces, and the confidence level is better than 99%. There are no significant differences between the counts on both surfaces within a 3 day culture, but the cell count on DLC coated TiNi on the sixth day is significantly higher than that on the TiNi. Although the growth rate of the cells is higher on DLC, the exponential growth and the well attachment and spreading of the cells show that both materials are compatible to the cell line and do not exhibit any cytotoxicity. A high nickel content in the TiNi films often causes suspicion of its suitability for medical use. However, as soon as the TiNi film is exposed to the ambient, oxygen and carbon are quickly adsorbed on the surface because titanium has a high affinity for oxygen and carbon. The presence of the  $\text{TiO}_2$  oxide layer (about 50 nm) on the TiNi film is beneficial to its corrosion resistance and biocompatibility [21].

#### 4. Summary

A TiNi/diamond-like-carbon (DLC) microcage for biological application has been designed, fabricated and characterized. A compressively stressed DLC film with a TiNi pattern on top expands and lifts the fingers upward once they are released from the substrate. A closing of the microcage is formed due to shape memory effect of the top TiNi film. The cage

can be opened/closed at controlling of the temperature below  $80^\circ\text{C}$ . Cell culture confirms that both TiNi and DLC films are biocompatible and cell friendly, no sign of cytotoxicity was observed toward the cell line used.

#### Acknowledgments

The financial support from the European FP6 project PROMENADE (project no 507965) and experimental help from Mr Fei Xie are acknowledged.

#### References

- [1] Pan C S and Hsu W Y 1997 *J. Micromech. Microeng.* **7** 7–13
- [2] Cecil J, Powell D and Vasquez D 2007 *Robot. Comput.- Integr. Manuf.* **23** 580–8
- [3] Volland B E, Heerlein H and Rangelow I W 2002 *Microelectron. Eng.* **61–62** 1015–23
- [4] Wierzbicki R, Houston K, Heerlein H, Barth W, Debski T, Eisenberg A, Menciassi A, Carrozza M C and Dario P 2006 *Microelectron. Eng.* **83** 1651–4
- [5] Luo J K, Flewitt A J, Spearing S M, Fleck N A and Milne W I 2005 *J. Micromech. Microeng.* **15** 1294
- [6] Fu Y Q, Du H J, Huang W M, Zhang S and Hu M 2004 *Sensors Actuators A* **112** 395–408
- [7] Miyazaki S and Ishida A 1999 *Mater. Sci. Eng. A* **275** 106–33
- [8] Kahn H, Huff M A and Heuer A H 1998 *J. Micromech. Microeng.* **8** 213–21
- [9] Grill A 1997 *Surf. Coat. Technol.* **94–95** 507
- [10] Robertson J 2002 *Mater. Sci. Eng. R* **R37** 129
- [11] Luo J K, He J H, Fu Y Q, Flewitt A J, Fleck N A and Milne W I 2005 *J. Micromech. Microeng.* **15** 1406–13
- [12] Luo J K, Huang R, He J H, Fu Y Q, Flewitt A J, Spearing S M, Fleck N A and Milne W I 2006 *Sensors Actuators A* **132** 346–53
- [13] Krulevitch P, Lee A P, Ramsey P B, Trevinon J C, Hamilton J and Northrup M A 1996 *J. Microelectromech. Syst.* **5** 270–82
- [14] Gill J J, Chang D T, Momoda L A and Carman G P 2001 *Sensors Actuators* **93** 148–56
- [15] Roch I, Bidaud P, Collard D and Buchaillot L 2003 *J. Micromech. Microeng.* **13** 330–6
- [16] Kohl M, Krevet B and Just E 2002 *Sensors Actuators* **97–8** 646–52
- [17] Fu Y Q, Luo J K, Flewitt A J, Ong S E, Zhang S, Du H J and Milne W I 2007 Micro-actuators of free-standing TiNiCu films *Smart Mater. Struct.* **16** 2651–7
- [18] Tsui Y C and Clyne T W 1997 *Thin Solid Films* **306** 23
- [19] Fu Y Q, Zhang S, Wu M J, Huang W M, Du H J, Luo J K, Flewitt A J and Milne W I 2006 *Thin Solid Films* **515** 80–6
- [20] Ishida A and Sato M 2003 *Acta Mater.* **51** 5571–8
- [21] Fu Y Q, Du H J, Zhang S and Huang W M 2005 *Mater. Sci. Eng. A* **403** 25–31